State-Space Modeling of DC Distribution Systems: Experimental Validation

Nils H. van der Blij[1], Laura M. Ramirez-Elizondo[1], Matthijs T.J. Spaan[2], Wuhua Li[3], and Pavol Bauer[1]

[1] Electrical Sustainable Energy, Delft University of Technology, The Netherlands

[2] Software Technology, Delft University of Technology, The Netherlands

[3] College of Electrical Engineering, Zhejiang University, China

***Abstract*—To tackle the challenges of future distribution systems, dc is being reconsidered. However, broad adoption of dc distribution systems requires additional research into the modeling, stability, protection and control of these systems. Previous research presents modeling methods that only consider monopolar configurations and do not take mutual couplings into account. Therefore, this paper presents a state-space method that can be applied to any dc distribution system, regardless of configuration and mutual couplings. Moreover, it shows how the state-space matrices can be derived in a programmatic manner. Furthermore, the models are validated using an experimental dc microgrid set-up. Due to the mathematical nature, the presented modeling method can be applied easily, and the stability and control can be analyzed algebraically.**

***Index Terms*—DC distribution, modeling, simulation, state-space**

I. Introduction

Growing energy demand and the introduction of distributed energy resources (DER) pose significant challenges for future distribution systems [1]. Firstly, the location of power generation will shift from areas of high consumption to areas of high resource availability [2]. Secondly, the power flow in these systems becomes bi-directional [3]. Thirdly, DER provide little to no inertia to the distribution system compared to conventional generation [4]. Lastly, the uncertainty in the grid is increased. Not only supply and demand are uncertain, but also the grid topology is uncertain as the distribution grid is being segmented into independent microgrids [5], [6].

DC distribution systems are being considered to tackle these challenges. This is because dc distribution systems are anticipated to have advantages with respect to efficiency, control, and the utilization of raw materials for converters [7], [8]. However, the broad adoption of dc systems still faces a strong market inertia of ac systems, a lack of standardization, and research with respect to the modeling, stability, protection and control [9].

Regardless, the adoption of dc systems is steadily increasing especially in niche applications such as data centers, telecommunications, commercial and residential buildings and street lighting [10]–[12].

This work was supported by the framework of the joint programming initiative ERA-Net Smart Grids Plus through the European Union's Horizon 2020 Research and Innovation Programme.

This paper has received funding from the European Union's Horizon 2020 Research and Innovation Programme under grant agreement No 734796.

Literature provides several methods for modeling dc distribution systems. Firstly, dc distribution systems can be modeled according to their transfer functions [13]–[15]. Secondly, a state-space representation of the system can be used [16]–[19]. Lastly, a specialized transient simulation environment can be employed [20]. However, the development of a transient simulation environment, which is focused and optimized on dc distribution systems, is still essential for the protection analysis of dc distribution systems. Furthermore, these modeling methods only consider monopolar configurations and, when extended to multiple phase conductors, do not take mutual couplings into account.

A non-transient state-space approach is used in this paper because of its computational efficiency, flexibility and simplicity. Literature presents a modeling method that enables the programmatic derivation of the state-space matrices from an incidence matrix [19]. However, the presented method is only applicable for monopolar dc grids, and therefore mutual couplings between multiple phase conductors are not taken into account.

The contributions of this paper are the presentation and experimental validation of a modeling method that allows for the analysis of any dc distribution system. It is shown how the state-space matrices of a dc distribution system with any number of nodes, distribution lines and phase conductors can be derived. Moreover, the state-space matrices can be derived programmatically, and the model takes the mutual couplings between phase conductors into account. Furthermore, the modeling method is validated using a dc microgrid set-up.

The mathematical nature of the presented modeling method has a couple of distinct advantages. Firstly, the method can be implemented in many simulation environments. Secondly, different systems can be analyzed in rapid succession. Thirdly, it allows for the algebraic analysis of, for example, stability and control of dc distribution systems.

The lumped element distribution line model utilized in this paper is valid when the wavelengths of the signals in the system are much longer than the physical length of the line. Therefore, the presented state-space model can be used for any dc system as long as this is the case.

This paper is organized as follows: in Section II the models for the distribution line, the dc distribution system and the power electronic converters are presented. In Section III the experimental set-up that is used in this paper is presented and the modeling method is validated. Lastly, in Section IV conclusions are drawn.

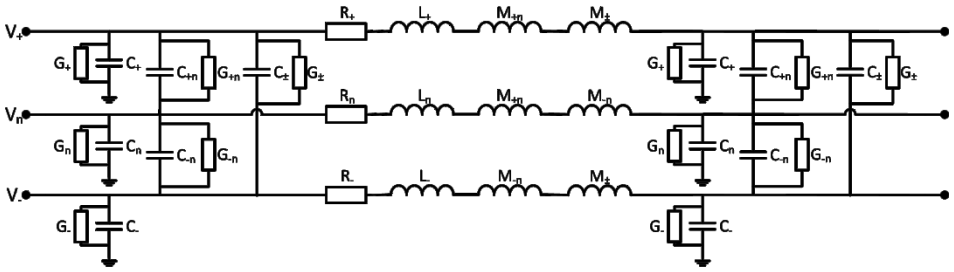

Fig. 1. Lumped element equivalent circuit of bipolar distribution lines including mutual coupling between phase conductors

II. DC Distribution System Model

DC distribution systems consist of power electronic converters, which are interconnected by distribution lines. In this paper the power electronic converters are modeled independently of the distribution system.

A. Distribution Line Model

Generally, transient models implemented in specialized transient simulation environments (such as PSCAD-EMTDC, EMTP and ATP) are more accurate than non-transient models. However, they are much more complex and require much more computational power and time for simulations.

Non-transient models often use a lumped element representation of the line. These lumped element models can be solved by utilizing transfer functions, differential equations or a state-space representation.

Lumped element models neglect propagation delays and frequency dependent effects. In general, lumped elements such as inductance, capacitance, resistance and conductance are frequency dependent. Furthermore, the validity of neglecting propagation delays depends on the wavelength of the signal

$$\lambda = \frac{c}{f\sqrt{\epsilon_r \mu_r}}, \tag{1}$$

where λ is the wavelength, f is the frequency, c is the speed of light, and ϵ_r and μ_r are the relatively permittivity and relative permeability of the medium respectively. Generally, propagation delays can be neglected if the wavelength of the signal is much larger than the length of the distribution line [21].

Previous research presents methods to model monopolar systems. However, ground currents are normally not permitted since they causes corrosion [22]. Furthermore, bipolar grids are becoming more common, which utilizes 3 parallel phase conductors. Therefore, in this paper, systems with multiple phase conductors are considered.

Different phase conductors have mutual couplings with each other in the form of mutual inductance, conductance and capacitance. These couplings can have a considerable effect on the dynamics of the dc system.

The distribution lines in this paper are modelled in a lumped element π configuration that includes mutual couplings between the phase conductors. The lumped element model for a bipolar distribution line is depicted in Fig. 1.

B. Distribution Network Model

Any dc distribution system can be described by its n nodes, l distribution lines, m phase conductors and o power electronic converters. An example of a dc distribution system, a microgrid, is shown in Fig. 2.

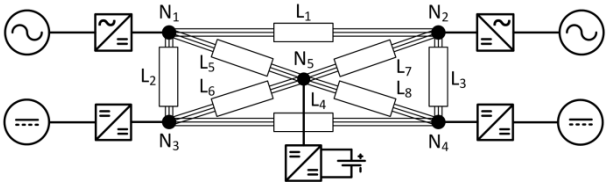

Fig. 2. Example of a bipolar dc microgrid system that contains storage, loads and sources

The state variables for the state-space model are chosen to be the voltages at each node and the currents in each line. The node voltages are dictated by the node capacitance and the net current into the node, while the line currents are dictated by the inductance of the line and the voltage over that inductance.

The net current flowing into each node consists of the currents from connected converters, currents in connected lines and the leakage current. The voltage over the inductance of the line consists of the voltage on each side of the line and the voltage drop over the resistance of the line. Therefore, the differential equations for the node voltages and line currents are given by

$$\boldsymbol{C}\dot{\boldsymbol{U}}_{\boldsymbol{N}} = \boldsymbol{I}_{\boldsymbol{N}} - \boldsymbol{\Gamma}^{\boldsymbol{T}}\boldsymbol{I}_{\boldsymbol{L}} - \boldsymbol{G}\boldsymbol{U}_{\boldsymbol{N}}\,, \tag{2}$$

$$\boldsymbol{L}\dot{\boldsymbol{I}}_{\boldsymbol{L}} = \boldsymbol{\Gamma}\boldsymbol{U}_{\boldsymbol{N}} - \boldsymbol{R}\boldsymbol{I}_{\boldsymbol{L}}\,, \tag{3}$$

where the boldface indicates a vector or a matrix. $\boldsymbol{U_N}$ are the voltages in each node, $\boldsymbol{I_L}$ are the currents in each line and $\boldsymbol{I_N}$ are the currents injected by converters into each node. Furthermore, the $\boldsymbol{C}$, $\boldsymbol{G}$, $\boldsymbol{L}$, and $\boldsymbol{R}$ depict the capacitance, conductance, inductance and resistance matrices of the system respectively. Moreover, the incidence matrix, $\boldsymbol{\Gamma}$, describes the interconnectivity of the system, and is given by

$$\boldsymbol{\gamma}(j,i) = \begin{cases} 1 & \text{if } I_j \text{ is flowing from node } i \\ -1 & \text{if } I_j \text{ is flowing to node } i \end{cases}, \tag{4}$$

$$\boldsymbol{\Gamma}\big((j-1)m+k,(i-1)m+k\big) = \boldsymbol{\gamma}(j,i)\,, \tag{5}$$

where the total number of nodes, lines and phase conductors are given by n, l and m respectively. Moreover, the indices i, j and k indicate a specific node, line, or phase conductor [23], [24].

To solve the differential equations of (2) and (3), these equations must be molded into the form of

$$\dot{\boldsymbol{x}} = \boldsymbol{A}\boldsymbol{x} + \boldsymbol{B}\boldsymbol{u}\,, \tag{6}$$
$$\boldsymbol{y} = \boldsymbol{D}\boldsymbol{x} + \boldsymbol{E}\boldsymbol{u}\,, \tag{7}$$

where $\boldsymbol{x}$ are the state variables, $\boldsymbol{u}$ are the input variables, $\boldsymbol{y}$ are the output variables, and $\boldsymbol{A}$, $\boldsymbol{B}$, $\boldsymbol{D}$ and $\boldsymbol{E}$ are the state-space matrices.

The state-space vectors for different phase conductors are grouped by node or line and are composed as

$$\boldsymbol{x} = \left[\, U_{1,1}\ U_{1,2}\ \ldots\ U_{n,m}\ \ I_{1,1}\ I_{1,2}\ \ldots\ I_{n,m} \,\right], \tag{8}$$
$$\boldsymbol{u} = \left[\, I_{N,1,1}\ I_{N,1,2}\ \ldots\ I_{N,l,m} \,\right], \tag{9}$$

where $U_{i,k}$ is the voltage of the k-th phase conductor at node i, $I_{j,k}$ is the current flowing in phase conductor k of line j and $I_{N,i,k}$ is the current injected into the k-th phase conductor of node i by, for example, power electronic converters.

The state space matrices ($\boldsymbol{A}$, $\boldsymbol{B}$, $\boldsymbol{D}$ and $\boldsymbol{E}$) can now be derived using (2) and (3) and are given by

$$\boldsymbol{A} = \begin{bmatrix} -\boldsymbol{C}^{-1}\boldsymbol{G} & -\boldsymbol{C}^{-1}\boldsymbol{\Gamma}^{\boldsymbol{T}} \\ \boldsymbol{L}^{-1}\boldsymbol{\Gamma} & -\boldsymbol{L}^{-1}\boldsymbol{R} \end{bmatrix}, \tag{10}$$
$$\boldsymbol{B} = \begin{bmatrix} -\boldsymbol{C}^{-1} \\ \emptyset \end{bmatrix}, \tag{11}$$
$$\boldsymbol{D} = \boldsymbol{I}\,, \tag{12}$$
$$\boldsymbol{E} = \emptyset\,, \tag{13}$$

where Ø indicates an empty matrix and $\boldsymbol{I}$ indicates an identity matrix.

The impedance ($\boldsymbol{L}$ and $\boldsymbol{R}$) and admittance matrices ($\boldsymbol{C}$, and $\boldsymbol{G}$) are formed using the impedance and admittance matrices of the distribution lines, which are given by

$$\boldsymbol{R}_{\boldsymbol{L},j} = \begin{bmatrix} R_1 & \cdots & 0 \\ \vdots & \ddots & \vdots \\ 0 & \cdots & R_n \end{bmatrix}, \tag{14}$$

$$\boldsymbol{L}_{\boldsymbol{L},j} = \begin{bmatrix} L_{11} & M_{12} & \cdots & M_{1m} \\ M_{21} & \ddots & \ddots & \vdots \\ \vdots & \ddots & \ddots & \vdots \\ M_{m1} & \cdots & \cdots & L_{mm} \end{bmatrix}, \tag{15}$$

$$\boldsymbol{C}_{\boldsymbol{L},j} = \begin{bmatrix} \sum_{k=1}^{m} C_{1k} & -C_{12} & \cdots & -C_{1m} \\ -C_{21} & \ddots & \ddots & \vdots \\ \vdots & \ddots & \ddots & \vdots \\ -C_{m1} & \cdots & \cdots & \sum_{k=1}^{m} C_{mk} \end{bmatrix}, \tag{16}$$

$$\boldsymbol{G}_{\boldsymbol{L},j} = \begin{bmatrix} \sum_{k=1}^{m} G_{1k} & -G_{12} & \cdots & -G_{1m} \\ -G_{21} & \ddots & \ddots & \vdots \\ \vdots & \ddots & \ddots & \vdots \\ -G_{m1} & \cdots & \cdots & \sum_{k=1}^{m} G_{mk} \end{bmatrix}. \tag{17}$$

Subsequently, since a π model is used, the capacitance and conductance matrices of each node can be found by summing half of the capacitance and conductance of each line connected to that node, such that

$$\boldsymbol{C}_{\boldsymbol{N},i} = \frac{1}{2}\sum_{j=1}^{l} \boldsymbol{C}_{\boldsymbol{L},j}\,[\boldsymbol{\gamma}(j,i) \neq 0]\,, \tag{18}$$

$$\boldsymbol{G}_{\boldsymbol{N},i} = \frac{1}{2}\sum_{j=1}^{l} \boldsymbol{G}_{\boldsymbol{L},j}\,[\boldsymbol{\gamma}(j,i) \neq 0]\,, \tag{19}$$

Furthermore, if any external capacitance (e.g., from connected converters) or conductance (e.g., grounding) is present in the network these can also be incorporated into $\boldsymbol{C}_{\boldsymbol{N},i}$ and $\boldsymbol{G}_{\boldsymbol{N},i}$ respectively.

Finally, the impedance and admittance matrices that are used in the state-space matrices are formed utilizing

$$\boldsymbol{C} = \begin{bmatrix} \boldsymbol{C}_{\boldsymbol{N},1} & \cdots & 0 \\ \vdots & \ddots & \vdots \\ 0 & \cdots & \boldsymbol{C}_{\boldsymbol{N},n} \end{bmatrix}, \tag{20}$$

$$\boldsymbol{G} = \begin{bmatrix} \boldsymbol{G}_{\boldsymbol{N},1} & \cdots & 0 \\ \vdots & \ddots & \vdots \\ 0 & \cdots & \boldsymbol{G}_{\boldsymbol{N},n} \end{bmatrix}, \tag{21}$$

$$\boldsymbol{L} = \begin{bmatrix} \boldsymbol{L}_{\boldsymbol{L},1} & \cdots & 0 \\ \vdots & \ddots & \vdots \\ 0 & \cdots & \boldsymbol{L}_{\boldsymbol{L},n} \end{bmatrix}, \tag{22}$$

$$\boldsymbol{R} = \begin{bmatrix} \boldsymbol{R}_{\boldsymbol{L},1} & \cdots & 0 \\ \vdots & \ddots & \vdots \\ 0 & \cdots & \boldsymbol{R}_{\boldsymbol{L},n} \end{bmatrix}. \tag{23}$$

C. Converter Model

The presented state-space modeling method allows for the utilization of any convenient converter model by employing the $\boldsymbol{I}_{\boldsymbol{N}}$ vector. Simplified diagrams of ac/dc, boost and buck converters are shown in Fig. 3. For most analyses, simple average, state-space models of these converters provide sufficient accuracy for the dynamic behavior of dc distribution systems.

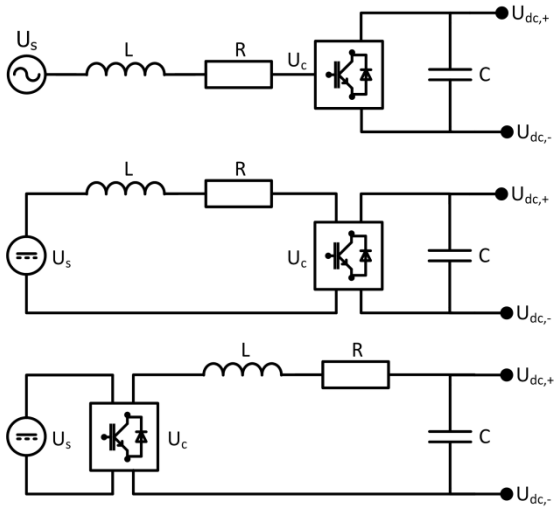

Fig. 3. Simplified diagrams of ac/dc, boost and buck converter

III. Experimental Validation

For the verification and validation of the state-space modeling method the experimental dc microgrid set-up shown in Fig. 4 is used. The set-up consists of four converters that, via a defined inductance and resistance, are connected to a dc bus. Furthermore, a relatively large resistor is connected to the dc bus to discharge the capacitors in the grid after operation.

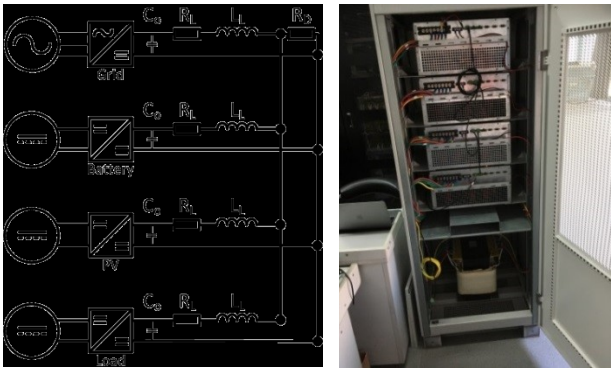

Fig. 4. Experimental DC microgrid set-up containing four power electronic converters that are connected to a dc bus.

The topology that is used for all the converters in the experimental set-up is shown in Fig. 5. The topology consists of three parallel half-bridges that can be operated as a bi-directional interleaved boost converter or as a three-phase ac/dc converter, depending on the control.

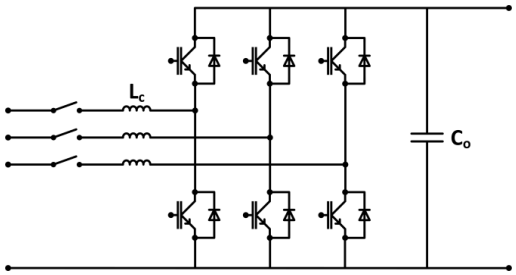

Fig. 5. Simplified topology of the power electronic converters in the experimental set-up.

Unless otherwise specified the converter parameters and the line parameters, connecting the different converters to the dc bus, are given by Table I.

TABLE I
Converter and Line Parameters

Converter	Parameters			
	L_c [mH]	C_o [mF]	R_L [Ω]	L_L [mH]
Grid	1.3	3.0	0.12	1.3
Battery	2.6	1.5	0.08	2.6
PV	2..6	1.5	0.08	2.6
Load	2.6	1.5	0.08	2.6

For the experiments that are conducted in this paper, one converter is connected to the main grid via an isolation transformer and is operated as a three-phase ac/dc converter, while the other converters are operated as dc/dc converters and are fed by a dc source.

A. Converter Models

For modeling the experimental dc microgrid, the state-space model described in the previous section is used. Furthermore, to model the converters a simple average model with an inner current controller, and outer voltage or power controller is used. The simplified model for the dc/dc converters is shown in Fig. 6.

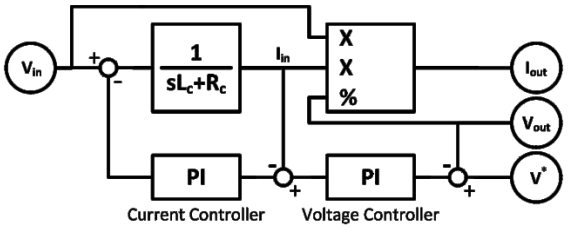

Fig. 6. Simplified converter and control model for the power electronic converters that is used in the simulations of the experimental set-up.

For the first experiment, the three-phase ac/dc converter (labeled as "Grid") is directly connected to the dc bus, while the other converters remain disconnected. Since the converter is connected directly to the grid R_L and L_L are negligible. The integral gain of the outer voltage controller is set to 0, while the proportional gain is set to 263 W/V. Therefore, the Grid converter operates as a droop converter.

The reference voltage of the Grid converter is initially 380 V and is stepped down to 361 V (0.95 p.u.) at t = 1 s, and back up again to 380 V at t = 3. The experimental and simulation results for the output voltage of the Grid converter are shown in Fig. 7.

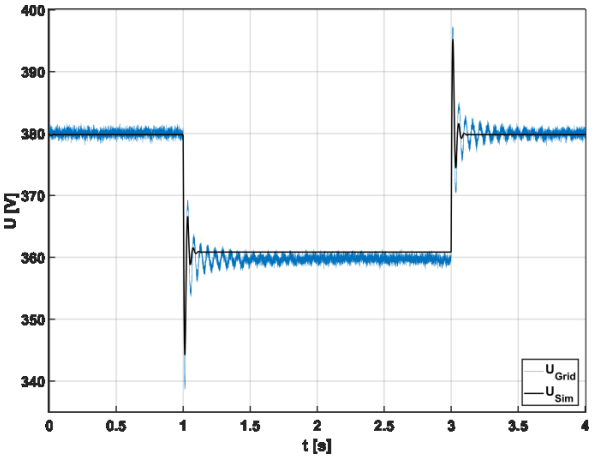

Fig. 7. Experimental and simulation results for when only the Grid converter is connected to the dc bus

The experimental results correspond relatively closely to the simulation results. However, the output voltage in the experiments is slightly more oscillatory, which is caused by the (unmodeled) PLL and discretization.

For the second experiment one of the dc/dc converters (labeled "PV") is also connected directly to the dc bus. Besides the steps in reference voltage of the Grid converter, the PV converter's output power is stepped up from 0 W to 3000 W at t = 7 s. The experimental and simulation results for the output voltage of the PV converter are shown in Fig. 8.

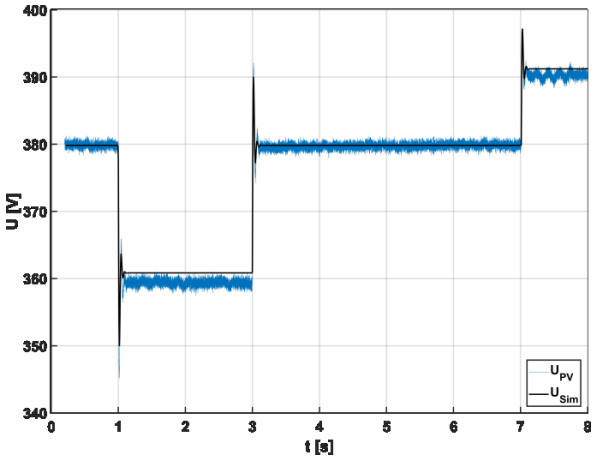

Fig. 8. Experimental and simulation results for when only the Grid and PV converters are connected to the dc bus

In this case the experimental and simulation results are congruent besides the slightly different steady state voltages. However, this is caused by the inaccuracy of the current and voltage sensors.

B. Full System Model

After the validation experiments for the ac/dc and dc/dc converter models, an experiment was done for the complete system. In this case all the converters (labeled "Grid", "Battery", "PV" and "Load") are connected to the dc bus with the parameters specified in Table I.

The Grid and Battery converters were operated as droop converters with a droop constant of 263 W/V, while the PV and Load converters were operated as a constant power source and constant power load respectively.

To test the system model under various conditions, the control set points of the converters were changed over time. The different set points over the duration of the experiment are given in Table II.

TABLE II
FULL SYSTEM VALIDATION SCENARIO

Time [s]	Control Set Points			
	Grid [U_0]	***Battery*** [U_0]	***PV*** [P]	***Load*** [P]
0.0	380 V	380 V	0	0
1.0	360 V	360 V	0	0
3.0	380 V	360 V	0	0
5.0	380 V	380 V	0	0
7.0	380 V	380 V	3.15 kW	0
9.0	380 V	380 V	3.15 kW	-3.30 kW

The results from the experiment and the simulation for the voltages at the converters' output capacitance are shown in Fig. 9.

It can be seen that there is strong congruency between the simulation and experimental results. Important to note is that the disturbances on the Grid converter's voltage were caused by harmonic interference in the grid.

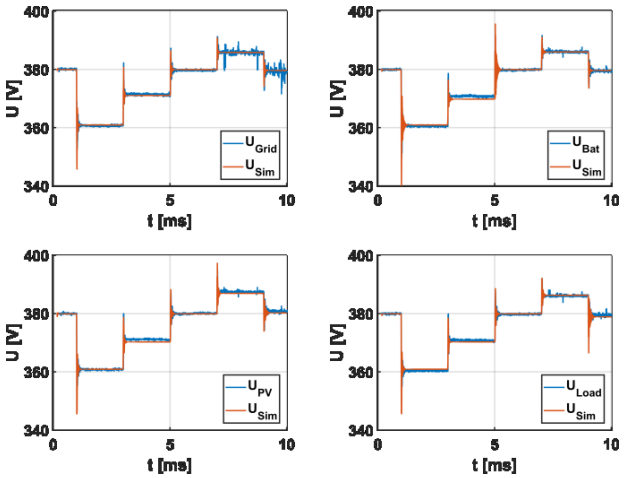

Fig. 9. Experimental and simulation results for the output voltages when all converters are connected to the dc bus

A more detailed look at the results for the Grid converter's output voltage is given in Fig. 10. Besides the influence of the harmonic interference at the end of the experiment the experimental results follow the simulation results closely.

An interesting observation is that the higher frequency oscillations, present in the simulations, are not as pronounced in the experiments. This is caused by the frequency dependence of the resistance in the dc bus bar and interconnections, which were not taken into account in the simulations.

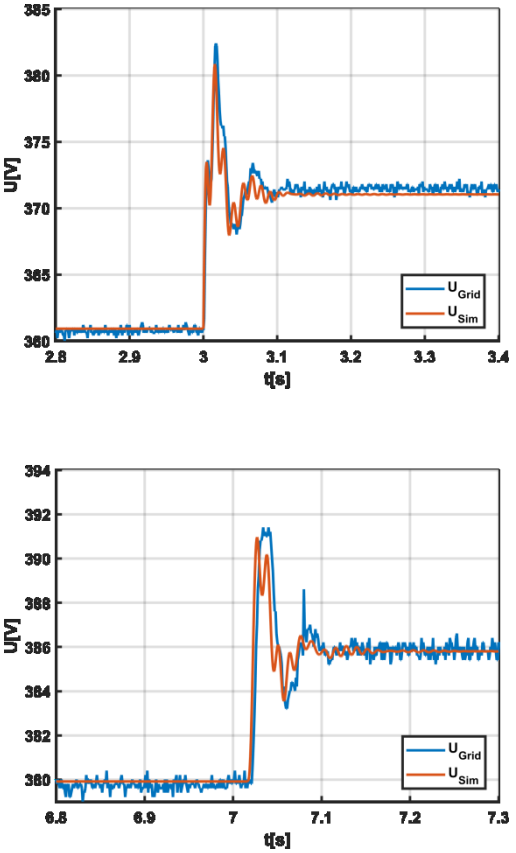

Fig. 10. Experimental and simulation results for the output voltages when all converters are connected to the dc bus

IV. Conclusions

Growing energy demand and the introduction of renewable energy resources pose significant challenges for distribution systems. To tackle these challenges dc distribution systems have been proposed, however more research is required on the modeling, stability, protection and control of these systems.

This paper presented a state-space modeling method that allows for the analysis of dc distribution systems, regardless of the number of nodes, distribution lines or phase conductors. Furthermore, it was shown how the system matrices can be derived programmatically and how the mutual couplings between phase conductors are taken into account.

The state-space modeling method was validated using an experimental dc microgrid set-up. Firstly, the simple converter models were verified. These models were shown to be accurate enough for system level analysis. Secondly, the modeling of the full system of four converters was validated. The simulation results showed strong congruency with the experimental results. An interesting observation was that the experimental results showed less oscillatory behavior because of the frequency dependency of the resistance in the grid.

In the future, the mathematical nature of the modeling method allows for it to be easily implemented in various simulation environments. Furthermore, different system configurations can be analyzed in swift succession. Additionally, the stability and control of dc distribution can be analyzed algebraically.

References

[1] A. Ipakchi and F. Albuyeh, "Grid of the future," in IEEE Power and Energy Magazine, vol. 7, no. 2, pp. 52-62, March-April 2009.

[2] J. Kim, S. Cho and H. Shin, "Advanced Power Distribution System Configuration for Smart Grid,", IEEE Transactions on Smart Grid, vol. 4, no. 1, pp. 353-358, 2013.

[3] L. Mackay, T. Hailu, L. Ramirez-Elizondo and P. Bauer, "Towards a DC distribution system - opportunities and challenges," IEEE First International Conference on DC Microgrids (ICDCM), 2015, pp. 215-220.

[4] J. Driesen and K. Visscher, "Virtual synchronous generators," 2008 IEEE Power and Energy Society General Meeting, 2008, pp. 1-3.

[5] N. Hatziargyriou, H. Asano, R. Iravani and C. Marnay, "Microgrids," in IEEE Power and Energy Magazine, vol. 5, no. 4, pp. 78-94, July-Aug. 2007.

[6] Flaih, Firas M. F. and Lin, Xiangning and Abd, Mohammed Kdair and Dawoud, Samir M. and Li, Zhengtian and Adio, Owolabi Sunday, "A new method for distribution network reconfiguration analysis under different load demands". Energies, vol. 10, no. 4, 2017.

[7] D. Marene Larruskain, Inmaculada Zamora, Oihane Abarrategui, Zaloa Aginako, Conversion of AC distribution lines into DC lines to upgrade transmission capacity, Electric Power Systems Research, Volume 81, Issue 7, Pages 1341-1348, 2011.

[8] T. Hakala, T. Lähdeaho and P. Järventausta, "Low-Voltage DC Distribution—Utilization Potential in a Large Distribution Network Company," in IEEE Transactions on Power Delivery, vol. 30, no. 4, pp. 1694-1701, Aug. 2015.

[9] L. Mackay, T. G. Hailu, G. C. Mouli, L. Ramírez-Elizondo, J. A. Ferreira and P. Bauer, "From DC nano- and microgrids towards the universal DC distribution system - a plea to think further into the future," IEEE Power & Energy Society General Meeting, 2015.

[10] A. T. Ghareeb, A. A. Mohamed and O. A. Mohammed, "DC microgrids and distribution systems: An overview," IEEE Power & Energy Society General Meeting, 2013.

[11] B. T. Patterson, "DC, Come Home: DC Microgrids and the Birth of the "Enernet"," in IEEE Power and Energy Magazine, vol. 10, no. 6, pp. 60-69, Nov.-Dec. 2012.

[12] Estefanía Planas, Jon Andreu, José Ignacio Gárate, Iñigo Martínez de Alegría, Edorta Ibarra. "AC and DC technology in microgrids: A review", Renewable and Sustainable Energy Reviews, Vol. 43, 2015, pp. 726-749

[13] A. P. N. Tahim, D. J. Pagano, E. Lenz and V. Stramosk, "Modeling and Stability Analysis of Islanded DC Microgrids Under Droop Control," in IEEE Transactions on Power Electronics, vol. 30, no. 8, pp. 4597-4607, 2015.

[14] T. Hailu, L. Mackay, L. Ramirez-Elizondo, J. Gu and J. A. Ferreira, "Voltage weak DC microgrid," International Conference on DC Microgrids (ICDCM), 2015.

[15] Q. Shafiee, T. Dragicevic, J. C. Vasquez and J. M. Guerrero, "Modeling, stability analysis and active stabilization of multiple DC-microgrid clusters," 2014 IEEE International Energy Conference (ENERGYCON), Cavtat, 2014, pp. 1284-1290.

[16] S. Anand and B. G. Fernandes, "Reduced-Order Model and Stability Analysis of Low-Voltage DC Microgrid," in IEEE Transactions on Industrial Electronics, vol. 60, no. 11, pp. 5040-5049, Nov. 2013.

[17] M. T. Dat, G. Van den Broeck and J. Driesen, "Modeling the dynamics of a DC distribution grid integrated of renewable energy sources," IECON 2014 - 40th Annual Conference of the IEEE Industrial Electronics Society, Dallas, TX, 2014, pp. 5559-5564.

[18] M. Karbalaye Zadeh, R. Gavagsaz-Ghoachani, J. Martin, S. Pierfederici, B. Nahid-Mobarakeh and M. Molinas, "Discrete-time modelling, stability analysis, and active stabilization of dc distribution systems with constant power loads," 2015 IEEE Applied Power Electronics Conference and Exposition (APEC), Charlotte, NC, 2015, pp. 323-329.

[19] P. B. S. Rodrigues and R. T. Pinto, "Dynamic Modelling and Control of VSC-Based Multi-Terminal DC Networks", 1st ed. Saarbrucken, Germany: Lambert Academic Publishing, 2012.

[20] Han, Joon; Oh, Yun-Sik; Gwon, Gi-Hyeon; Kim, Doo-Ung; Noh, Chul-Ho; Jung, Tack-Hyun; Lee, Soon-Jeong and Kim, Chul-Hwan. "Modeling and Analysis of a Low-Voltage DC Distribution System". Resources, vol 4, no 3, pp. 713-735.

[21] C. R. Paul, "Analysis of Multiconductor Transmission Lines", 2nd ed. New York, NY, USA: Wiley, 2007.

[22] J. J. Justo, F. Mwasilu, J. Lee, and J.-W. Jung, "Ac-microgrids versus dc-microgrids with distributed energy resources: A review," Renew. Sustain. Energy Rev., vol. 24, pp. 387–405, 2013.

[23] N. H. van der Blij, L. M. Ramirez-Elizondo, M. T. J. Spaan and P. Bauer, "A State-Space Approach to Modelling DC Distribution Systems," in IEEE Transactions on Power Systems, vol. 33, no. 1, pp. 943-950, Jan. 2018.

[24] N. H. van der Blij, L. M. Ramirez-Elizondo, M. T. J. Spaan and P. Bauer, "Symmetrical Component Decomposition of DC Distribution Systems," in IEEE Transactions on Power Systems, vol. 33, no. 3, pp. 2733-2741, May 2018.